Free energy landscape and cooperatively rearranging region in a hard sphere glass

Takashi Yoshidome,* Akira Yoshimori, and Takashi Odagaki
Department of Physics, Kyushu University, Fukuoka 812-8581, Japan
(Received 13 April 2007; published 23 August 2007)

Exploiting the density functional theory, we calculate the free energy landscape (FEL) of the hard sphere glass in three dimensions. From the FEL, we estimate the number of the particles in the cooperatively rearranging region (CRR). We find that the density dependence of the number of the particles in the CRR is expressed as a power law function of the density. Analyzing the relaxation process in the CRR, we also find that the string motion is the elementary process for the structural relaxation, which leads to the natural definition of the simultaneously rearranging region as the particles displaced in the string motion.

DOI: 10.1103/PhysRevE.76.021506 PACS number(s): 64.70.Pf

I. INTRODUCTION

Understanding of the glass transition has amazingly advanced in last two decades because of intensive theoretical, experimental and computational studies [1–6]. Among several views for the glass transition, the free energy landscape (FEL) picture [7–9] provides a unified understanding of the characteristics of the glass transition. The FEL is a function of a particle configuration $\{\mathbf{R}_i\}$ and is given by the free energy calculated from the phase space around $\{\mathbf{R}_i\}$ [8,9]. The system is assumed to move on the FEL which has many basins near T_g. Here, we refer to a basin as a region in which all configurations are relaxed to the same minimum [3]. The FEL picture provides a phenomenological understanding of the dynamical properites [10–14] and the specific heat anomaly [15–19] near T_g. It is, therefore, important to construct explicitly the FEL using the microscopic Hamiltonian in order to proceed to quantitative analysis of the glass transition. In this paper, we construct the FEL of the hard sphere glass in three dimensions with the thermodynanic potential of the density functional theory [7].

In addition to the FEL, the cooperatively rearranging region (CRR) proposed by Adam and Gibbs [20] is also an important concept to understand the glass transition. Adam and Gibbs [20] have succeeded in describing the Vogel-Fulcher temperature dependence of the shear viscosity $\eta(T)$ [21,22]. In their theory, the structural relaxation is caused by the rearrangement of particles in the CRR [20]. The number of the particles in the CRR N_{CRR} increases as the temperature is reduced toward T_g. The Vogel-Fulcher behavior is attributed to the temperature dependence of $N_{\mathrm{CRR}}(T)$. With $N_{\mathrm{CRR}}(T)$, $\eta(T)$ can be expressed $\eta(T) \propto \exp[N_{\mathrm{CRR}}(T)\Delta E/(k_B T)]$, where ΔE is the activation energy for a particle, assumed to be independent of the temperature T. Because $N_{\mathrm{CRR}}(T)$ increases as T is reduced, $\eta(T)$ deviates from the Arrhenius temperature dependence. In order to test their theory, it is important to give a microscopic definition of the CRR and to find its dependence on the parameters such as the temperature and the density. In view of the success of the FEL picture, it is necessary to relate the CRR to the structure of the FEL in order to give a microscopic definition of the CRR.

In the previous papers [7,8], we showed that a microscopic definition of the CRR naturally emerges from the structure of the FEL. In the Adam-Gibbs theory, the structural relaxation is assumed to be caused by the rearrangement of particles in the CRR [20]. In the FEL picture, on the other hand, the structural relaxation corresponds to the transition from one of the basins to the adjacent basin [7–9]. The number of the particles needed for the transition to the adjacent basin is not the all particles in the system but a several particles. These particles are thus considered as those in the CRR proposed by Adam and Gibbs [20]. These particles are also those displaced cooperatively at the excited state between the two adjacent basins.

From the structure of the FEL, we also proposed a new rearranging region, the simultaneously rearranging region (SRR) which is the difference between two adjacent basins [7,8]. The difference between these two basins is given by the position of a few particles at the local minima. The exchange of position of these particles brings the representative point from one basin to the other.

In order to discuss the validity of the Adam and Gibbs theory, thus, it is desirable to estimate N_{CRR} from the FEL. In this paper, we propose a method to estimate N_{CRR} from the FEL. We show that one can estimate N_{CRR} by calculating the FEL for the particles confined in a spherical shell of fixed particles. In order to demonstrate the usefulness of the method, we study N_{CRR} of the hard sphere glass in three dimensions. We will obtain the density dependence of N_{CRR}. We also investigate the structural relaxation process in the CRR. We show that the string motion in which several particles displace like a billiard is the elementary process of the structural relaxation.

We organize this paper as follows: We first present a method to calculate the FEL with the thermodynamic potential of the density functional theory in Secs. II and III. A method to estimate N_{CRR} is given in Sec. IV. In Sec. V, we show the FEL, SRR, density dependence of N_{CRR}, and the structural relaxation process in the CRR. Summary is given in Sec. VI.

II. CONSTRUCTION OF THE FREE ENERGY LANDSCAPE

In the previous paper [7], we proposed that the free energy as a function of $\{\mathbf{R}_i\}$ can be obtained with the thermo-

*t-yoshidome@iae.kyoto-u.ac.jp

dynamic potential of the density functional theory [23–27]. In this theory, the grand potential $\Omega[\rho(\mathbf{r})]$ is treated as a functional of the density field $\rho(\mathbf{r})$. In order to express $\Omega[\rho(\mathbf{r})]$ as a function of $\{\mathbf{R}_i\}$, we employ a sum of Gaussians as the density field [24,26]:

$$\rho_G(\mathbf{r}) = \left(\frac{\alpha}{\pi}\right)^{3/2} \sum_i \exp[-\alpha(\mathbf{r}-\mathbf{R}_i)^2]. \tag{1}$$

Here α and $\mathbf{R}_i$ are the degree of the spread of the density distribution and the average position of the ith particle, respectively. The density field (1) means that the distribution of the motion around $\{\mathbf{R}_i\}$ is approximated by Gaussian functions. Namely, the motion within $|\mathbf{r}-\mathbf{R}_i| \leqslant 1/\sqrt{\alpha}$ is coarse-grained by α. With Eq. (1), $\Omega[\rho(\mathbf{r})]$ becomes a function of α and $\{\mathbf{R}_i\}$:

$$\Omega(\alpha,\{\mathbf{R}_i\}) \equiv \Omega[\rho_G(\mathbf{r})]. \tag{2}$$

We use this grand potential for calculation of the FEL [7,8].

III. RAMAKRISHNAN AND YUSSOFF FREE ENERGY FUNCTIONAL

We employ the free energy functional developed by Ramakrishnan and Yussoff for $\Omega[\rho(\mathbf{r})]$ [28,29]. This free energy functional has been used for the study of the liquid-crystal transition [26,30] and the glass transition [31–40] of the hard sphere system. In this section, we explain their expression of the free energy functional briefly. Detail is explained in the reviews of the density functional theory [24,26,27].

One can first obtain the exact free energy functional for an ideal gas $\Omega_{\mathrm{id}}[\rho(\mathbf{r})]$. Here, the ideal gas means that the Hamiltonian H_N is given by $H_N=K$, where K is the kinetic energy. The free energy functional for the ideal gas is represented by

$$\Omega_{\mathrm{id}}[\rho(\mathbf{r})] = k_B T \int d\mathbf{r}\rho(\mathbf{r})\{\ln[\rho(\mathbf{r})\Lambda^3]-1\} + \mu \int d\mathbf{r}\rho(\mathbf{r}), \tag{3}$$

where Λ is the thermal de Broglie wavelength and μ is the chemical potential.

In order to obtain the free energy functional for the objective system, Ramakrishnan and Yussouff [28,29] expanded $\Psi[\rho(\mathbf{r})] \equiv \Omega_{\mathrm{id}}[\rho(\mathbf{r})] - \Omega[\rho(\mathbf{r})]$ in a functional Taylor series about the uniform density $\bar{\rho} \equiv \frac{1}{V}\int d\mathbf{r}\rho(\mathbf{r})$. It is important to expand not the full free energy functional $\Omega[\rho(\mathbf{r})]$ but only $\Psi[\rho(\mathbf{r})]$. This ensures that $\Omega_{\mathrm{id}}[\rho(\mathbf{r})]$ is treated to all orders in the density. Expanding $\Psi[\rho(\mathbf{r})]$ in a functional Taylor series about $\bar{\rho}$, $\Psi[\rho(\mathbf{r})]$ becomes

$$\Psi[\rho(\mathbf{r})] = \Psi[\bar{\rho}] + \sum_{n=1}^{\infty} k_B T \int d\mathbf{r}_1 \cdots d\mathbf{r}_n c_n(\mathbf{r}_1 \cdots \mathbf{r}_n) \times \Delta\rho(\mathbf{r}_1)\cdots\Delta\rho(\mathbf{r}_n). \tag{4}$$

Here, $\Delta\rho(\mathbf{r}) = \rho(\mathbf{r}) - \bar{\rho}$, and $c_n(\mathbf{r}_1 \cdots \mathbf{r}_n)$ is the nth direct correlation function at the uniform density $\bar{\rho}$, which is defined by

$$c_n(\mathbf{r}_1 \cdots \mathbf{r}_n) \equiv \frac{\beta\delta^n\Psi[\rho]}{\delta\rho(\mathbf{r}_1)\cdots\delta\rho(\mathbf{r}_n)}. \tag{5}$$

Thus, $\Omega[\rho(\mathbf{r})]$ becomes

$$\Omega[\rho(\mathbf{r})] = \Omega_{\mathrm{id}}[\rho(\mathbf{r})] - \Psi[\bar{\rho}] - \sum_{n=1}^{\infty} k_B T \times \int d\mathbf{r}_1 \cdots d\mathbf{r}_n c_n(\mathbf{r}_1 \cdots \mathbf{r}_n)\Delta\rho(\mathbf{r}_1)\cdots\Delta\rho(\mathbf{r}_n). \tag{6}$$

By using Eq. (6), the difference between the grand potential of the crystal and that of liquid can be obtained

$$\beta\Delta\Omega[\rho(\mathbf{r})] \equiv \beta\Omega[\rho(\mathbf{r})] - \beta\Omega[\bar{\rho}] = \int_V d\mathbf{r}\rho(\mathbf{r})\ln\left[\frac{\rho(\mathbf{r})}{\bar{\rho}}\right] - \frac{1}{2}\int_V d\mathbf{r}_1 \int_V d\mathbf{r}_2 c_2(|\mathbf{r}_1-\mathbf{r}_2|)[\rho(\mathbf{r}_1)-\bar{\rho}] \times [\rho(\mathbf{r}_2)-\bar{\rho}], \tag{7}$$

where the expansion is truncated in the second order. In addition, since one can shown that c_1 is constant [24,27], the first order of the expansion becomes 0. The direct correlation function $c_2(r)$ can be calculated with the equilibrium liquid theory [23]. We use the Percus-Yevick approximation for the direct correlation function of the hard sphere [23].

IV. THE CRR OF THE HARD SPHERE GLASS

One can estimate N_{CRR} by investigating whether the transition to the adjacent basin takes place or not when several particles in the system are fixed. Consider the two adjacent basins in the FEL. The number of the particles for transition to the adjacent basin requires cooperative motion of the particles in the CRR. Hence even if the particles which do not displace during the transition to the adjacent basin are fixed, the system can also transit to the adjacent basin. The number of the particles in the CRR N_{CRR} corresponds to the smallest number of the unfixed particles. In the following, we first present the procedure for obtaining the configuration of the hard sphere. Then the method to estimate N_{CRR} is explained.

We first prepare the random packing of hard sphere made by the infinitesimal gravity protocol, whose algorithm is described in Refs. [41,42]. The number density $\rho_0\sigma^3$ is 1.04, where σ is the diameter of the hard sphere. Hereafter, the position of the particles at $\rho_0\sigma^3=1.04$ is denoted by $\{\mathbf{R}_i^0\}$. We obtain the position of the particles $\{\mathbf{R}_i\}$ at the objective density $\rho\sigma^3$ as follows:

$$\mathbf{R}_i = \left(\frac{\rho_0\sigma^3}{\rho\sigma^3}\right)\mathbf{R}_i^0. \tag{8}$$

When we estimate N_{CRR}, we first constrain the particles in the spherical shell made by fixing the particles (Fig. 1), assuming that the shape of the CRR is a sphere. We first set the inner diameter of the spherical shell to 6σ. In order to obtain $\{\mathbf{R}_i\}$ at the minimum in the basin, the particles in the confin-

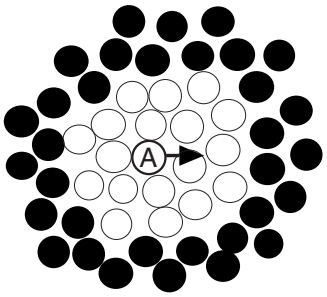

FIG. 1. A schematic representation of the model under consideration. *A* is the particle which we force to move. The black particles are fixed.

ing area are relaxed to minimize $\Omega(\alpha,\{\mathbf{R}_i\})$ in the $\{\mathbf{R}_i\}$ space. We exploit the steepest decent method for minimization, whose algorithm is explained in the Appendix.

In order to estimate N_{CRR}, we calculate the FEL for a process in which we force to displace a particle *A* which is near the center of the spherical shell (Fig. 1). Other particle's $\{\mathbf{R}_i\}$ are relaxed to minimize $\Omega(\alpha,\{\mathbf{R}_i\})$ in the $\{\mathbf{R}_i\}$ space with the position of the particle *A* fixed. Then we judge whether the transition to the adjacent basin takes place or not with the procedure explained later. If the transition takes place, we decrease the size of the confining area and calculate the FEL in the new confining area. As the number of particles in the confined area N_{trap} is reduced, the transition to the adjacent basin cannot take place at a certain critical number. This critical number is N_{CRR}.

We judge whether the transition to the adjacent basin takes place or not with the following procedure. We first relax $\{\mathbf{R}_i\}$ at each point of the calculated FEL to the minimum in the basin. Then we compare the obtained $\{\mathbf{R}_i\}$ with that at the initial state. Hereafter we use $\{\mathbf{R}_i^{\mathrm{min}}\}$ and $\{\mathbf{R}_i^{\mathrm{initial}}\}$ for $\{\mathbf{R}_i\}$ at the minimum in the basin and that at the initial state, respectively. If $\{\mathbf{R}_i^{\mathrm{min}}\}$ for all the point of the calculated FEL are coincide with $\{\mathbf{R}_i^{\mathrm{initial}}\}$, there is one basin which corresponds to the initial basin, and otherwise, more than two basins exist. In the latter case, transition to the adjacent basin takes place.

Finally, since the positions of the particles are distributed around $\{\mathbf{R}_i\}$ with the width of $\sigma/\sqrt{\alpha}$, we assume that the two particles do not overlap when $|\mathbf{R}_i-\mathbf{R}_j| \geqslant \sigma-\sigma/\sqrt{\alpha}$. If one can find only the initial basin by displacing the particle *A* as far as possible, the transition to the adjacent basin does not take place.

V. RESULTS

In principle, one can calculate the FEL in α and $\{\mathbf{R}_i\}$ space with the grand potential (2). The shape of the FEL depends on α. In the limit of $\alpha \to 0$ where the degree of the coarse-graining $1/\sqrt{\alpha}$ becomes ∞, the FEL becomes uniform, and thus $\rho_G(\mathbf{r})$ (1) is independent of $\{\mathbf{R}\}$. In the limit of $\alpha \to \infty$ where the degree of the coarse graining $1/\sqrt{\alpha}$ becomes 0, on the other hand, the FEL becomes the same as the potential energy landscape.

In the present paper, we show the FEL at a certain value of α, $\alpha\sigma^2=36$. The corresponding root mean square displacement of the particle around the center of the Gaussian function is $1/\sqrt{\alpha} \sim 0.17\sigma$. This value is close to the root mean square displacement of the particle around the FCC lattice at the liquid-crystal transition point, which is approximately 0.19σ [30].

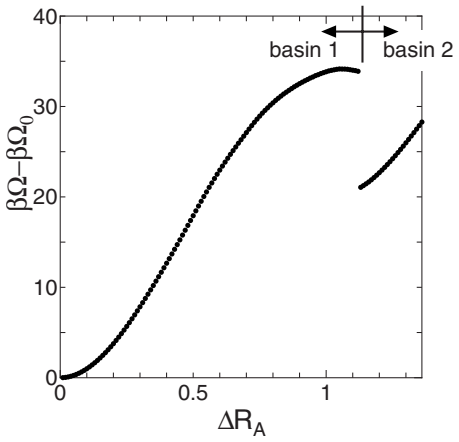

FIG. 2. The FEL for $\rho\sigma^3=0.963$, $N_{\mathrm{trap}}=18$, and $\alpha\sigma^2=36$. The horizontal axis is the displacement of the forced particle. The vertical axis is the difference between Ω at ΔR_A and Ω at the initial particle configuration.

A. Free energy landscape and SRR

Figure 2 shows the FEL as a function of the displacement of the forced particle *A*, ΔR_A, at $\rho\sigma^3=0.963$. The number of the particles in the spherical shell N_{trap} is set to 18. As the particle *A* is forced to displace, $\Omega(\alpha,\{\mathbf{R}_i\})$ increases. For $1.05\sigma \leqslant \Delta R_A \leqslant 1.12\sigma$, $\Omega(\alpha,\{\mathbf{R}_i\})$ is decreased approximately $0.3k_BT$. Then the abrupt decrement of $\Omega(\alpha,\{\mathbf{R}_i\})$ takes place at $\Delta R_A=1.13\sigma$.

The abrupt decrement of $\Omega(\alpha,\{\mathbf{R}_i\})$ at $\Delta R_A=1.13\sigma$ is caused by the large displacement of particle labeled by *B* in Fig. 3. When $\Delta R_A \leqslant 1.12\sigma$, all particles except for the particle *A* displace short distance. However, at $\Delta R_A=1.13\sigma$, the particle *B* displaces significantly. Other particles displace short distance. The large displacement of the particle *B* is caused by the steepest decent method. When we calculate the FEL, $\{\mathbf{R}_i\}$ are relaxed to minimize $\Omega(\alpha,\{\mathbf{R}_i\})$ in the $\{\mathbf{R}_i\}$ space with the position of the forced particle *A* fixed. In the case of $\Delta R_A \leqslant 1.12\sigma$, since the system is near the local minimum, the particle *B* displaces short distance due to the relaxation. [see Fig. 4(a)]. At $\Delta R_A=1.13\sigma$, on the other hand, since the system is far from the local minimum, the particle *B* displaces long distance due to the relaxation [Fig. 4]. Thus, the large displacement of the particle *B* occurs at $\Delta R_A=1.13\sigma$.

By relaxing $\{\mathbf{R}_i\}$ at each point of the calculated FEL to the minimum in the basin, we find that in the case of $\Delta R_A \leqslant 1.12\sigma$, the system belongs to the initial basin (basin 1). Otherwise, the system belongs to the different basin (basin 2). The configurations at the minimum of basin 1 and basin 2 are shown in Fig. 5. By relaxing $\{\mathbf{R}_i\}$ at $\Delta R_A > 1.12\sigma$, the particle *B* goes to the position of the particle *A* at $\Delta R_A=0$. In addition, the particle *A* goes to the position of the particle *B*

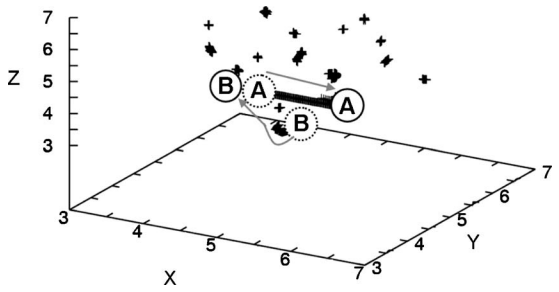

FIG. 3. The structural relaxation of the particles in the confining area. The points are the calculated result of the trajectories of the particles. Dotted spheres represent the particles at $\Delta R_A=0$, and solid spheres represent the particles at $\Delta R_A=1.36\sigma$. The arrows mark the paths of the positions of two particles. *A* is the particle which we force to displace.

at $\Delta R_A=0$. Namely, the configuration at the minimum of basin 2 is that the two particles are exchanged mutually from the configuration at the minimum of basin 1. The positions of other particles in basin 2 coincide with those in basin 1. Thus, the simultaneously rearranging region (SRR) consists of 2 particles. Since there are two basins, the transition to the adjacent basin occurs at $N_{\mathrm{trap}}=18$.

In order to estimate the lower limit of N_{CRR} at $\rho\sigma^3=0.963$, we reduce the confining area and calculate the FEL. Figure 6 shows the FEL for $N_{\mathrm{trap}}=9$ and $\rho\sigma^3=0.963$. Here, we calculate the FEL within $\Delta R \leqslant 0.35$, because the assumption $|\mathbf{R}_i-\mathbf{R}_j| \geqslant \sigma-\sigma/\sqrt{\alpha}$ is not satisfied in the case of $\Delta R \geqslant 0.36$. By relaxing $\{\mathbf{R}_i\}$ at each point of the calculated FEL

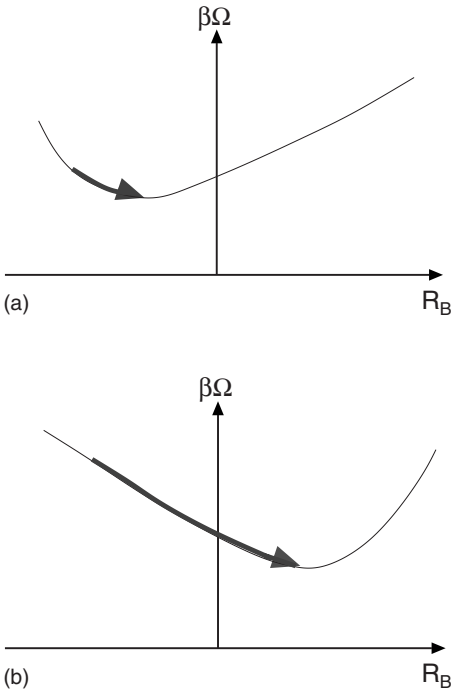

FIG. 4. The schematic representations of the relaxation to the minimum of $\Omega(\alpha,\{\mathbf{R}_i\})$ in the $\{\mathbf{R}_i\}$ space. (a) at $\Delta R_A \leqslant 1.12\sigma$ in Fig. 2, and (b) at $\Delta R_A=1.13\sigma$ in Fig. 2. We represent the FEL in one dimension for simplicity. The system relaxes to the minimum along the arrow.

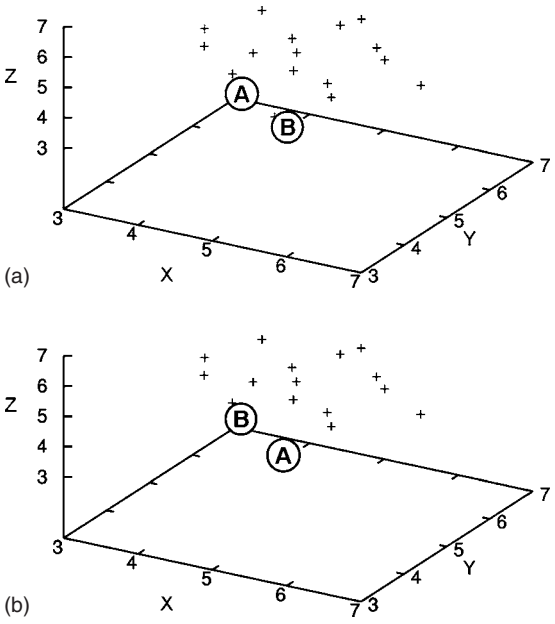

FIG. 5. The configurations at the minimum in the basin 1 (a) and that at the minimum in the basin 2 (b). Points show $\{\mathbf{R}_i\}$ of particles. Two spheres A, B are the particles exchanged mutually their positions.

to the minimum in the basin, we find only the initial basin. Thus, the transition to the adjacent basin does not occur at $N_{\mathrm{trap}}=9$. Namely, N_{CRR} is larger than 9, and thus N_{CRR} is between 10 and 18 at $\rho\sigma^3=0.963$.

B. Density dependence of the number of the particles in the CRR

Figure 7 shows the density dependence of N_{CRR} at $\alpha\sigma^2=36$. The number of the particles in the CRR N_{CRR} is increased as the density is raised. It reaches approximately 50 at $\rho\sigma^3=1.12$. The density dependence of N_{CRR} can be expressed by the power law (see Fig. 7). By extrapolating to the high density with the power law fit, we find that N_{CRR}

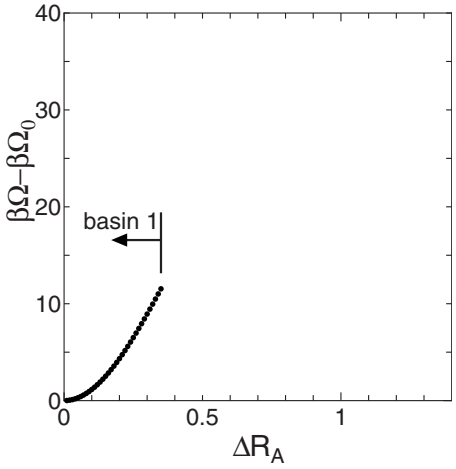

FIG. 6. The FEL for $\rho\sigma^3=0.963$ and $N_{\mathrm{trap}}=9$. The horizontal axis and vertical axis are the same as those in Fig. 2.

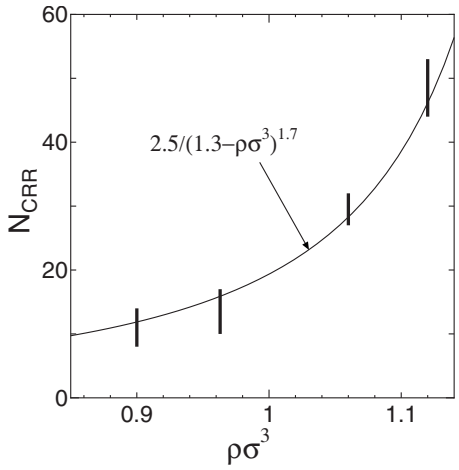

FIG. 7. The density dependence of the size of the CRR, N_{CRR} for the hard sphere glass at $\alpha\sigma^2=36$. The horizontal axis is the density, and the vertical axis is N_{CRR}. For each density, the lower and upper limit of N_{CRR} are connected by the bar. The solid line represents the power-law fit.

becomes infinity at $\rho\sigma^3=1.3$. The exponent of the power law is 1.7.

According to the Adam and Gibbs theory [20], N_{CRR} becomes infinity at the Vogel-Fulcher density. Thus, $\rho\sigma^3=1.3$ corresponds to the Vogel-Fulcher density for the hard sphere glass. The corresponding packing fraction is 0.68, which corresponds to the random closed packing $\eta_{RCP}=0.64-0.68$. This result suggests that the Vogel-Fulcher density corresponds to the random closed packing.

C. Structural relaxation in the CRR: String motion

The elementary process of structural relaxation takes place within the CRR because the particles in the CRR are needed for the structural relaxation. As explained in Sec. I, the structural relaxation corresponds to the transition to the adjacent basin in the FEL picture. In order to clarify the elementary process of the structural relaxation, thus, we investigate the structural relaxation in the CRR of Fig. 3.

From Fig. 3, we find that the structural relaxation is produced by large displacement of two particles. Two particles

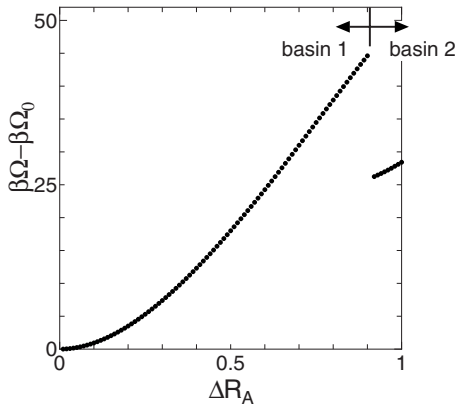

FIG. 8. The FEL at $\rho\sigma^3=1.06$, $N_{\mathrm{trap}}=32$, and $\alpha\sigma^2=36$. The horizontal axis and vertical axis are same as those in Fig. 2.

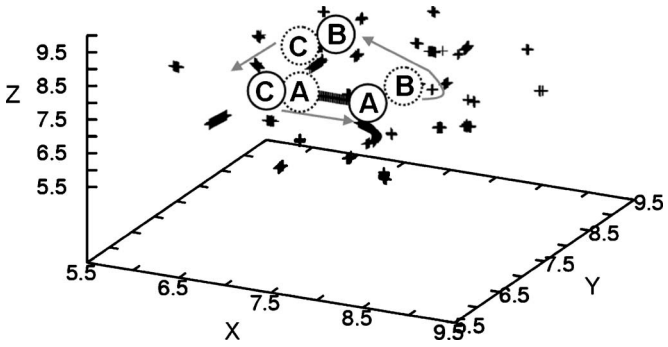

FIG. 9. The structural relaxation of the particles in the confining area. The points are the calculated result of the trajectories of the particles. Dotted spheres represent the partices at $\Delta R_A=0$, and solid spheres represent the particles at $\Delta R_A=1.0\sigma$. The arrows mark the paths of three particles A, B, and C. A is the particle which we force to displace.

displace similar to billiard balls, and the exchanges of their position take place. This motion is a string motion. The particles displaced in the string motion are those in the SRR. Other particles keep their relative positions.

The string motion occurs for other densities. In Fig. 8, we first show the FEL for $N_{\mathrm{trap}}=32$, which is the upper limit of N_{CRR} at $\rho\sigma^3=1.06$ (see Fig. 7). The qualitative behavior of the FEL is the same as the FEL in Fig. 2, such as the increasing of $\Omega(\alpha,\{\mathbf{R}_i\})$ and the abrupt decrease of $\Omega(\alpha,\{\mathbf{R}_i\})$. The transition to the adjacent basin occurs at $\Delta R_A=0.92\sigma$. Figure 9 shows the structural relaxation during the change of $\Omega(\alpha,\{\mathbf{R}_i\})$ in Fig. 8. The exchange of three particles takes place. We also confirmed that the qualitative behavior of the FEL and the structural relaxation takes place for other densities.

The string motion also occurs for other α. We first show the the FEL for $N_{\mathrm{trap}}=10$, which is the upper limit of N_{CRR} at $\alpha\sigma^2=3$ and $\rho\sigma^3=0.963$. This value of $\alpha\sigma^2$ is close to that at the liquid-amorphous solid transition point [43]. The qualitative behavior of the FEL is the same as the FELs in Figs. 2 and 8. The transition to the adjacent basin occurs at $\Delta R_A=0.62\sigma$. Figure 11 shows the structural relaxation during the change of $\Omega(\alpha,\{\mathbf{R}_i\})$ in Fig. 10. The exchange of five particles takes place.

The string motion has been observed in molecular dynamics (MD) simulations [44–47]. For example, Miyagawa *et al.* observed simultaneous exchange of four particles in the MD simulation of three-dimensional (3D) binary soft-sphere mixture [44]. The structural relaxation in the CRR is qualitatively same as that observed by Miyagawa *et al.* [44]. However, Glotzer *et al.* have observed the string motion in quasi-one-dimensional paths [45–47], which is different behavior from our result of the string motion. The string motion in quasi-one-dimensional paths is expected to be obtained by changing the shape of the confining area such as the cuboid cell.

VI. SUMMARY AND DISCUSSION

In this paper, we have studied the FEL for hard sphere glass in three dimensions by the density functional theory.

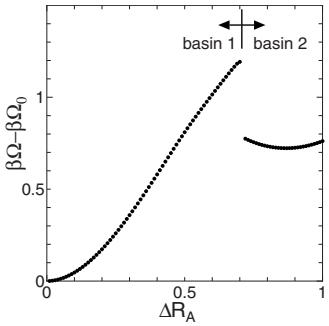

FIG. 10. The FEL for $\rho\sigma^3=0.963$, $N_{\mathrm{trap}}=10$, and $\alpha\sigma^2=3$. The horizontal axis and vertical axis are same as those in Fig. 2.

We have obtained three results: FEL, number of the particles in the CRR N_{CRR}, and the elementary process of the structural relaxation.

We have first obtained the FEL as a function of the displacement of the particle ΔR_A. To this end, we calculate the FEL in which we force to displace a selected particle which is near the center of the spherical shell (Fig. 1). Other particle's $\{\mathbf{R}_i\}$ are relaxed to minimize $\Omega(\alpha,\{\mathbf{R}_i\})$ in the $\{\mathbf{R}_i\}$ space with the position of the forced particle fixed. The FEL is increased as the selected particle is displaced. Then the abrupt decrease of $\Omega(\alpha,\{\mathbf{R}_i\})$ occurs by the large displacement of the several particles. When the abrupt decrease of $\Omega(\alpha,\{\mathbf{R}_i\})$ occurs, the transition to the adjacent basin occurs.

When we calculate the FEL, we have set $\alpha\sigma^2=36$ corresponding to the mean squared displacement of the particle in an fcc structure at the melting point. Although the value of $\alpha\sigma^2$ should be determined from the first principle, there are no method to determine the value of $\alpha\sigma^2$ at present. We do not consider that we have to employ the value of $\alpha\sigma^2$ at the free energy minimum [31,37–40]. However, the aim of the present study is to demonstrate that one can calculate the FEL and the CRR of the hard sphere glass with the density functional theory. Thus, we employ $\alpha\sigma^2=36$ for simplicity. It is the future study to determine the value of $\alpha\sigma^2$ from the first principle.

In the present paper, we have used the the Percus-Yevick approximation for the direct correlation function [23]. It is, however, well known that the Percus-Yevick approximation is less accurate at high densities for hard sphere system [23]. For this reason, the Verlet-Weis correction to the Percus-Yevick approximation has been used at high density [52,53]. However, we confirmed that the difference between the free energy calculated with the Percus-Yevick approximation and that calculated with the Verlet-Weis correction is small at $\alpha\sigma^2=36$. Thus we expect that the present results do not change if we employ the Verlet-Weis correction of the Percus-Yevick approximation.

By decreasing the size of the confining area, we have estimated N_{CRR}. By fitting the density dependence of N_{CRR} with power law function of the density, we have found that the Vogel-Fulcher density is $\rho\sigma^3=1.3$. The corresponding packing fraction is 0.68, which corresponds to the random close packing fraction. Thus, the Vogel-Fulcher density corresponds to the packing fraction of the random close packing.

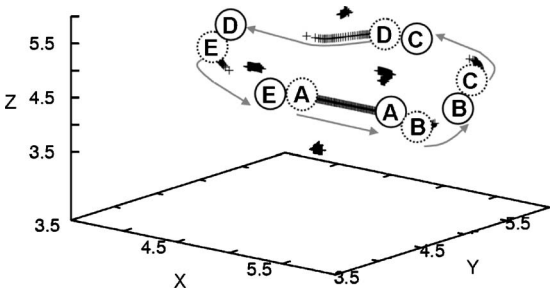

FIG. 11. The structural relaxation of the particles in the confining area. The points are the calculated result of the trajectories of the particles. Dotted spheres represent the particles at $\Delta R_A=0$, and solid spheres represent the particles at $\Delta R_A=1.0\sigma$. The arrows mark the paths of five particles is shown by arrows. "A" is the particle which we force to displace.

According to the theoretical and numerical studies for the hard spheres in three dimensions [49–51], there is a Kauzman packing fraction between 0.58 and 0.62. This packing fraction is lower than our result, 0.68. We believe that our result is more natural than others, because our result indicates that the Kauzmann packing fraction corresponds to the random packing fraction. However, since the discrepancy might come from the value of $\alpha\sigma^2$, we need to check the present results by calculating the FEL and CRR with the value of $\alpha\sigma^2$ obtained from the first principle in the future.

The present results are considered to be independent of the algorithm chosen. In the present paper, we have employed the infinitesimal gravity protocol to prepare the random packing of hard sphere [41,42]. There are, however, several algorithms to generate random packing of hard sphere [54–56]. If the structures of the random packing of the hard sphere depend on the algorithm chosen, the size of the CRR would change. Thus, we compare the pair correlation function $g(r)$ obtained from each algorithm and our algorithm. The minor difference is found in the shape of the second peak. We expect that the present results do not change from such a minor difference and thus, we consider that the present results do not depend on the algorithm chosen.

We have found that the string motion is the elementary process for structural relaxation. This motion is also observed in the MD simulations [44–48]. We have also found that the particles displaced in the string motion correspond to the particles in the SRR.

The study with another shape of the confining area is the future problem. The string motion which is similar to ring motion (Figs. 3, 9, and 11) might be changed if the another shape of the confining area is employed. For example, if we constrain the particles in the ellipsoid with large aspect rate, the string motion in quasi-one-dimensional paths would be obtained. In the future we will study the FEL, the CRR, and the string motion with another shape of the confining area.

ACKNOWLEDGMENTS

This work was supported in part by the Grant-in-Aid for

Scientific Research from the Ministry of Education, Culture, Sports, Science and Technology.

APPENDIX

In relaxation of particles, we employ the steepest decent method. With this method, one can relax the particles to the minimum of $\Omega(\alpha,\{\mathbf{R}_i\})$ with the positions of particle A fixed. Suppose we have a configuration $\{\mathbf{R}_i^{\text{old}}\}=(x_1^{\text{old}},y_1^{\text{old}},z_1^{\text{old}},\ldots,z_N^{\text{old}})$. With the gradient of $\Omega(\alpha,\{\mathbf{R}_i\})$ with respect to $\{\mathbf{R}_i\}$, we relax the ith particle as follows:

$$x_i^{\text{new}} = x_i^{\text{old}} - \delta \left. \frac{\partial[\beta\Omega(\alpha,\{\mathbf{R}_i\})]}{\partial x_i} \right|_{x_i=x_i^{\text{old}}}. \tag{A1}$$

Here, x_i^{new} is the position of the ith particle in the x direction after the relaxation (A1). In addition, δ is the constant small value. The relaxation (A1) is also employed both in the y and z directions. When the relaxation (A1) is performed all particles except for particle A, one can obtain a configuration $\{\mathbf{R}_i^{\text{new}}\}=(x_1^{\text{new}},y_1^{\text{new}},z_1^{\text{new}},\ldots,z_N^{\text{new}})$. By substitute $\{\mathbf{R}_i^{\text{new}}\}$ into $\{\mathbf{R}_i^{\text{old}}\}$, we repeat the relaxation (A1) until the particles are relaxed to the minimum of $\Omega(\alpha,\{\mathbf{R}_i\})$.

[1] M. Goldstein, J. Chem. Phys. **51**, 3728 (1969).
[2] W. Götze in *Liquids, Freezing and Glass Transition*, edited by J. P. Hansen *et al.* (North-Holland, Amsterdam, 1989) p. 287.
[3] F. H. Stillinger, Science **267**, 1935 (1995).
[4] M. Mézard and G. Parisi, J. Chem. Phys. **111**, 1076 (1999).
[5] D. J. Wales *Energy Landscapes* (Cambridge University Press, Cambridge, 2004).
[6] F. Sciortino, J. Stat. Mech.: Theory Exp. 2005, P05015 (2005).
[7] T. Yoshidome, A. Yoshimori, and T. Odagaki, J. Phys. Soc. Jpn. **75**, 0504005 (2006).
[8] T. Odagaki, T. Yoshidome, A. Koyama, and A. Yoshimori, J. Non-Cryst. Solids **352**, 4843 (2006).
[9] T. Odagaki and T. Ekimoto, J. Non-Cryst. Solids (to be published).
[10] T. Odagaki and Y. Hiwatari, Phys. Rev. A **41**, 929 (1990).
[11] T. Odagaki, J. Matsui, and Y. Hiwatari, Phys. Rev. E **49**, 3150 (1994).
[12] T. Odagaki, Phys. Rev. Lett. **75**, 3701 (1995).
[13] T. Odagaki, Prog. Theor. Phys. Suppl. **126**, 9 (1997).
[14] M. Higuchi and T. Odagaki, J. Phys. Soc. Jpn. **66**, 3134 (1997).
[15] T. Tao, A. Yoshimori, and T. Odagaki, Phys. Rev. E **64**, 046112 (2001).
[16] T. Tao, A. Yoshimori, and T. Odagaki, Phys. Rev. E **66**, 041103 (2002).
[17] T. Odagaki, T. Tao, and A. Yoshimori, J. Non-Cryst. Solids **307-310**, 407 (2002).
[18] T. Odagaki, T. Yoshidome, T. Tao, and A. Yoshimori, J. Chem. Phys. **117**, 10151 (2002).
[19] T. Tao, T. Odagaki, and A. Yoshimori, J. Chem. Phys. **122**, 044505 (2005).
[20] G. Adam, and J. H. Gibbs, J. Chem. Phys. **43**, 139 (1965).
[21] H. Vogel, Phys. Z. **22**, 645 (1921).
[22] G. S. Fulcher, J. Am. Ceram. Soc. **8**, 339 (1925).
[23] J. P. Hansen and L. R. Mcdonald, *Theory of Simple Liquids* (Academic Press, London, 1986).
[24] D. Oxtoby, in *Liquids, Freezing and Glass Transition*, edited by J. P. Hansen *et al.* (North-Holland, Amsterdam, 1989) p. 145.
[25] R. Evans, *Fundamentals of Inhomogeneous Fluids*, edited by D. Henderson (Dekker, New York, 1992), p. 85.
[26] Y. Singh, Phys. Rep. **207**, 351 (1992).
[27] A. Yoshimori, J. Theor. Comput. Chem. **3**, 117 (2004).
[28] T. V. Ramakrishnan and M. Yussouff, Phys. Rev. B **19**, 2775 (1979).
[29] A. D. J. Haymet and D. W. Oxtoby, J. Chem. Phys. **74**, 2559 (1981).
[30] J. L. Barrat, J. P. Hansen, G. Pastore, and E. W. Waisman, J. Chem. Phys. **86**, 6360 (1987).
[31] Y. Singh, J. P. Stoessel, and P. G. Wolynes, Phys. Rev. Lett. **54**, 1059 (1985).
[32] C. Dasgupta, Europhys. Lett. **20**, 131 (1992).
[33] C. Dasgupta and O. T. Valls, Phys. Rev. E **58**, 801 (1998).
[34] C. Dasgupta and O. T. Valls, Phys. Rev. E **59**, 3123 (1999).
[35] C. Dasgupta and O. T. Valls, J. Phys.: Condens. Matter **12**, 6553 (2000).
[36] X. Xia and P. G. Wolynes, Proc. Natl. Acad. Sci. U.S.A. **97**, 2990 (2000).
[37] C. Kaur and S. P. Das, Phys. Rev. Lett. **86**, 2062 (2001).
[38] C. Kaur and S. P. Das, J. Phys.: Condens. Matter **13**, 7259 (2001).
[39] K. Kim and T. Munakata, Phys. Rev. E **68**, 021502 (2003).
[40] S. P. Singh and S. P. Das, J. Non-Cryst. Solids **352**, 4857 (2006).
[41] T. Okubo and T. Odagaki, J. Phys.: Condens. Matter **16**, 6651 (2004).
[42] R. Ogata, T. Odagaki, and K. Okazaki, J. Phys.: Condens. Matter **17**, 4531 (2005).
[43] T. Yoshidome, A. Yoshimori, and T. Odagaki (unpublished).
[44] H. Miyagawa, Y. Hiwatari, B. Bernu, and J. P. Hansen, J. Chem. Phys. **86**, 3879 (1988).
[45] C. Donati, J. F. Douglas, W. Kob, Steven J. Plimpton, P. H. Poole, and S. C. Glotzer, Phys. Rev. Lett. **80**, 2338 (1998).
[46] S. C. Glotzer, J. Non-Cryst. Solids **274**, 342 (2000).
[47] Y. Gebremichael, M. Vogel, and S. C. Glotzer, J. Chem. Phys. **120**, 4415 (2004).
[48] Y. Gebremichael, M. Vogel, M. N. J. Bergroth, and S. C. Glotzer, J. Phys. Chem. B **109**, 15068 (2005).
[49] R. J. Speedy, Mol. Phys. **95**, 169 (1998).
[50] G. Parisi and F. Zamponi, J. Chem. Phys. **123**, 144501 (2005).
[51] L. Angelani, G. Foffi, and F. Sciortino, J. Phys.: Condens. Matter **19**, 256207 (2007).
[52] L. Verlet and J. J. Weis, Phys. Rev. A **5**, 939 (1972).
[53] D. Henderson and E. W. Grundke, J. Chem. Phys. **63**, 601 (1975).
[54] C. Bennett, J. Appl. Phys. **43**, 2727 (1972).
[55] B. D. Lubachevsky and F. H. Stillinger, J. Stat. Phys. **60**, 561 (1990); **64**, 501 (1991).
[56] L. E. Silbert, D. Ertas, G. S. Grest, T. C. Halsey, and D. Levine, Phys. Rev. E **65**, 031304 (2002).